Research Article Vol. 60, No. 3 / 20 January 2021 / Applied Optics 533

applied optics

Mitigation of laser-induced contamination in vacuum in high-repetition-rate high-peak-power laser systems

Zbyněk Hubka,[1,2,*] Jakub Novák,[1] Irena Majerová,[1] Jonathan T. Green,[1] Praveen K. Velpula,[1] Robert Boge,[1] Roman Antipenkov,[1] Václav Šobr,[1] Daniel Kramer,[1] Karel Majer,[1] Jack A. Naylon,[1] Pavel Bakule,[1] and Bedřich Rus[1]

[1]ELI Beamlines, Institute of Physics, Czech Academy of Sciences, Na Slovance 2, 18221 Prague, Czech Republic
[2]Czech Technical University in Prague, Faculty of Nuclear Sciences and Physical Engineering, Břehová 7, 115 19 Prague, Czech Republic
*Corresponding author: zbynek.hubka@eli-beams.eu

Received 12 November 2020; revised 14 December 2020; accepted 15 December 2020; posted 16 December 2020 (Doc. ID 414878); published 11 January 2021

Vacuum chambers are frequently used in high-energy, high-peak-power laser systems to prevent deleterious nonlinear effects, which can result from propagation in air. In the vacuum sections of the Allegra laser system at ELI-Beamlines, we observed degradation of several optical elements due to laser-induced contamination (LIC). This contamination is present on surfaces with laser intensity above 30 GW/cm^2 with wavelengths of 515, 800, and 1030 nm. It can lead to undesired absorption on diffraction gratings, mirrors, and crystals and ultimately to degradation of the laser beam profile. Because the Allegra laser is intended to be a high-uptime source for users, such progressive degradation is unacceptable for operation. Here, we evaluate three methods of removing LIC from optics in vacuum. One of them, the radio-frequency-generated plasma cleaning, appears to be a suitable solution from the perspective of operating a reliable, on-demand source for users.

https://doi.org/10.1364/AO.414878

1. INTRODUCTION

It is quite common for large portions of high-energy high-power lasers to be in vacuum in order to avoid problems with nonlinear effects like self-focusing or self-phase modulation [1,2]. The components in such vacuum systems must be chosen carefully to avoid contamination of optical surfaces under vacuum. Degassing of materials or contamination in an optical system can pose a risk for optics by creation of an adsorbed layer on it. While optical surface quality can degrade in air due to the accumulation of layers of contamination [3], their growth is much more pronounced in vacuum environments. The need to remove these layers from optics has been known since the beginning of the satellite programs [4]. Wide use of synchrotrons generating extreme UV in the 1980s and 1990s showed that the growth of these layers is strongly linked with a presence of UV or x-ray radiation [5–9]; this phenomenon is often called "radiation-induced contamination" or "laser-induced contamination" (LIC).

The source of this contamination is mostly low-vapor-pressure hydrocarbon molecules present in vacuum chambers, which are difficult to remove with vacuum pumps. These molecules dissociate by photon-induced ionization (called cracking) and deposit a carbonaceous layer on the optical surfaces. The growth mechanism of this contamination has been previously modeled [10,11].

Hydrocarbon contamination degrades the performance of optical components, which is a problem in scanning electron microscopy [12], lithography [13], or spacecraft systems using lasers with UV wavelengths [14–16]. It has also been shown that the LIC can degrade the performance of laser systems with wavelengths outside the UV region [3,17] through multiphoton absorption process and can lead to laser-induced damage [10,17,18]. Two examples of optical components from a laser system with visible LIC spots are shown in Fig. 1 and support the idea of LIC being caused by multiphoton absorption at 1030 nm.

Methods to remove the LIC from optical surfaces aim to create ionized molecules and radicals, which bond to the molecules deposited on the contaminated surface (often carbon) and generate volatile molecules (water vapor, CO_x, NO_x, etc.), which can be removed from the chamber by vacuum pumps. One of the common methods uses gaseous oxygen in combination with UV radiation (either from an external source or the laser/synchrotron itself) [12,16,19] to generate ozone or oxygen radicals, which help break down the contamination layers. Other methods include generating radicals through radio-frequency discharge [8,20] or ablating the contamination layers

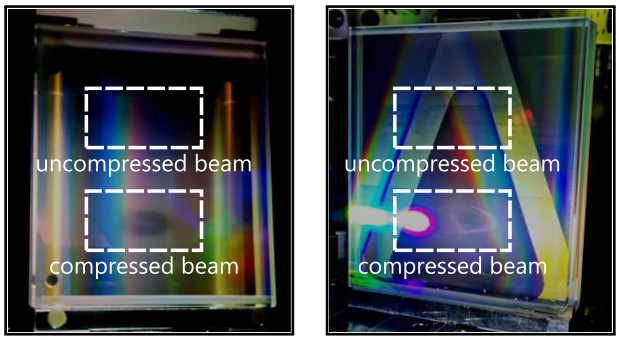

Fig. 1. Laser-induced contamination spots on two dielectric gratings from two similar pulse compressors. LIC is visible only in the area where the compressed pulse hits the grating. The laser pulse parameters are 1030 nm, 3 ps, 15 mm $1/e^2$ diameter, and 200 mJ energy. (a) Grating with a darkening in the bottom part. (b) Different grating with similar contamination, with extra white edges visible due to a different camera angle. The bright white saturated area in (b) next to the LIC comes from the flashlight used to illuminate the grating.

with laser radiation [21]. Although more common in systems with UV and x-ray wavelengths, short-pulse near-infrared lasers can also suffer from LIC. Here, we describe how LIC affects the performance of the Allegra laser and how it can be mitigated *in situ* allowing high uptime for the laser source.

Allegra is a high-repetition-rate, high-energy, high-average-power, ultrashort pulse laser intended to be used for laser-driven x-ray and XUV light source experiments [22]. The system is based on picosecond optical parametric chirped pulse amplification (OPCPA) and is designed to generate 100 mJ, sub 15 fs pulses at 1 kHz.

To avoid nonlinear effects in air, we placed a large portion of the system inside vacuum, including three diffraction grating-based Treacy compressors, three second-harmonic (SHG) stages, three OPCPA sections, and a series of chirped mirrors for final pulse compression. The laser system is designed for user operation with maximum uptime, and significant attention is given to its stability, high reliability, and automation [23–25]. Because of the high demands for operation, it is not reasonable to regularly remove optics from carefully aligned optical systems in vacuum for cleaning. To maintain the maximum possible uptime, cleaning must be performed *in situ* with minimal disturbance to the laser.

Although there are other laser systems within ELI-Beamlines with similar laser pulse intensities but lower repetition rates (10 Hz and lower), under similar vacuum conditions, it is only the 1 kHz Allegra laser that has observed beam degradation due to LIC, indicating that the repetition rate is an important factor in developing the contamination layers.

A. LIC in Allegra Laser System

After a given period of laser operation, typically five days of operation at 20 mJ output (10^7 shots), we begin to notice changes in the laser performance and can observe LIC on optics in vacuum (typical pressure reached in our chambers is $\sim 10^{-6}$ mbar) in both broadband amplification stages as well as in the pump pulse compressors. It is represented by a darkening, with bright edges

Table 1. Fluence and Intensity of Laser Pulse with Different Wavelengths on Optical Surfaces inside Vacuum Chamber and Presence of LIC Spots[a]

Wavelength	Pulse Duration	Fluence	Intensity	LIC Visible
1030 nm	0.5 ns	260 mJ/cm^2	0.5 GW/cm^2	no
1030 nm	3 ps	260 mJ/cm^2	87 GW/cm^2	yes
515 nm	3 ps	113 mJ/cm^2	38 GW/cm^2	yes
750–920 nm	3 ps	6.5 mJ/cm^2	2.2 GW/cm^2	no
750–920 nm	15 fs	6.5 mJ/cm^2	430 GW/cm^2	yes

[a]Repetition rate of laser pulses is 1 KHz.

from certain viewing angles, as shown in Fig. 1. The spots are the same size as the laser beam (~15 mm@$1/e^2$) and have the shape of a donut, with the middle part being lighter in color, similar to what was previously observed [16,18,26]. To capture them on a camera can be quite challenging, as the spots are usually visible only from a narrow range of angles.

From our experience, the presence of LIC spots is closely correlated to the laser pulse intensity rather than pulse fluence, as we only observe LIC on optics where the laser pulses are compressed and see nothing where those same pulses are stretched. This indicates the higher the laser pulse intensity is, the faster LIC accumulates up to the point where it is visible with the naked eye (see Table 1 for details). The visual presence of darkened LIC spots on mirrors, OPCPA and SHG crystals, and diffraction gratings degrades their performance by introducing absorption. Contaminated gratings also suffer from increased diffraction into the 0th order.

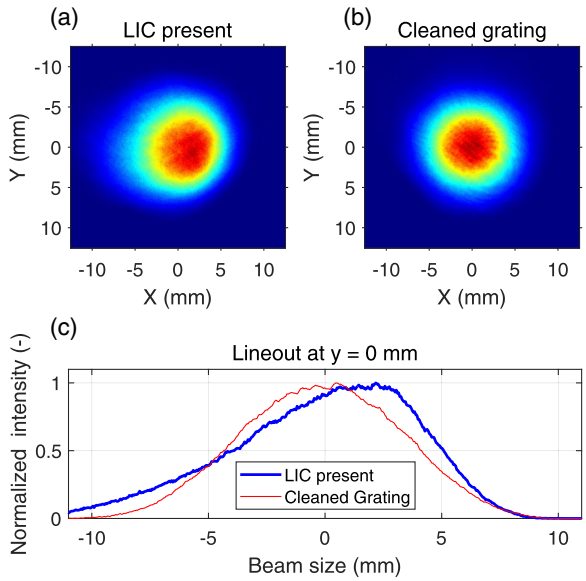

Fig. 2. Comparison of the 1030 nm Treacy compressor output beam profile before and after 12 h of cleaning the vacuum chamber with the RF plasma source. (a) Distorted beam profile with contaminated optics present in the compressor. (b) Undistorted beam profile after cleaning the chamber with an RF plasma source overnight. (c) Beam profile lineout at the center. The source of distortion might be related to the asymmetric absorption on the grating with LIC present (data in Fig. 8) or to a different setpoint of active beam-pointing stabilization system, causing a slightly different overlap of the laser beam and LIC, present on the optics in the chamber.

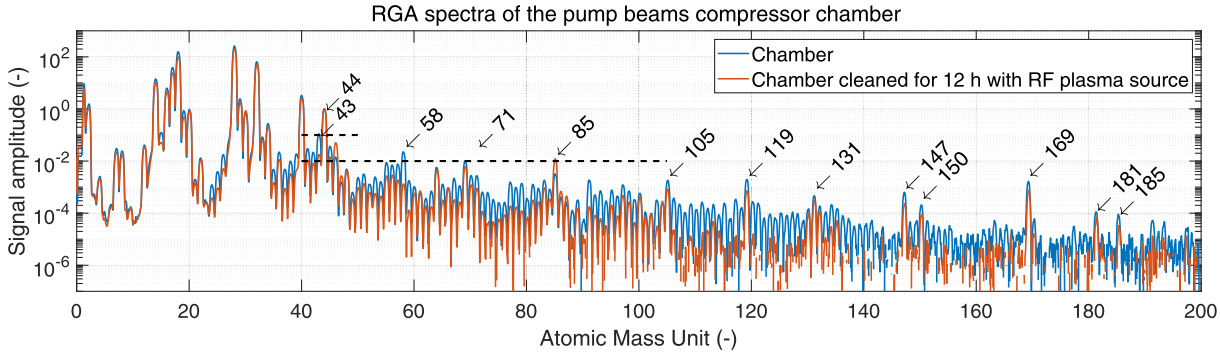

Fig. 3. RGA spectra of the pump pulse compressor chamber, both measured at $\sim 10^{-6}$ mbar. Both data sets are normalized to the atomic mass units (amu) 44 peak. The blue data set was measured one day after the chamber was evacuated; the orange data set after 12 h or running the RF plasma source. After the cleaning, in most cases, the amplitude of the peaks above 100 amu decreased by almost an order of magnitude. Despite this visible improvement, the presence of peaks at amu 71, 85, 105, 119, 131, 147, 150, 169, 181, and 185 still suggests some level of contamination in the chamber.

If not eliminated, these LIC spots can lead to undesirable losses of energy inside the system and eventually to catastrophic failure through laser-induced damage. In our case, the spot on the left grating in Fig. 1 caused the efficiency of the grating diffraction to drop by 13% and to the creation of distorted beam profiles, visible in Fig. 2.

B. Possible Sources of Contamination

We have made efforts to keep our vacuum chambers as clean as possible and use vacuum-compatible materials such as stainless steel, aluminum, and Kapton and Teflon materials with vacuum-compatible lubricants. All components placed into the chambers are ultrasonically cleaned. The chambers are evacuated using turbomolecular pumps with dry screw vacuum pumps for prevacuum. Flanges and doors are sealed using unbaked Viton O-rings.

When looking at typical residual gas analyzer (RGA) spectra of our pump laser compressor chamber in Fig. 3, we can compare two traces. In the first one, the chamber was vented, opened, and evacuated again. The second trace is after cleaning the chamber for 12 h with an RF plasma source, which greatly improves the situation. The ratio between the amplitude of the peaks with amu 44 (CO_2) and amu 43 (hydrocarbon C_3H_7) is below 1/10, and the amplitude of peaks above amu 44 is $\leq$1/100 of the amu 44 peak, which is in accordance with the laser interferometer gravitational-wave observatory (LIGO) standard [27].

Both RGA spectra show concentrations of hydrocarbon constituents, indicated by groups of peaks separated by 14 amu related to CH_2 as well as multiple peaks with amu >100. The peak with amu 58 is usually caused by the Viton O-rings used on all the doors and flanges. The peaks with amu 119, 131, 147, 150, 169, or 185 are most probably linked with the use of perfluoropolyether-based grease, and their amplitude is not getting much smaller after the RF plasma cleaning process. That can be explained by the absence of hydrocarbons in this type of grease. Other peaks and the hydrocarbon groups in Fig. 3 might be linked to the hydrocarbon-based ultrahigh vacuum grease used in the past and to the fact that our chambers were cleaned with vacuum wipes soaked in acetone and isopropyl-alcohol immediately after the manufacturing process. Contamination from the wipes is supported by Fourier-transform infrared spectroscopy tests from the walls showing clear presence of polyester molecules.

2. METHODS OF REMOVING LIC FROM OPTICS

We have tested the following three methods to eliminate LIC from our optics: UV-ozone cleaning, laser pulse cleaning, and RF plasma cleaning. We used three nonidentical contaminated mirrors from a different laser, the Ti:sapphire section of a Prague Asterix laser system [28], with different degrees of contamination. The following results were obtained in a small, dedicated vacuum chamber with the contaminated mirrors facing the cleaning device/beam at an angle of 45 deg. All of the methods successfully removed the LIC from the optical surface, and their specifics are described below.

A. UV-ozone Cleaning

For this cleaning method, we used atmospheric pressure inside the small chamber and mounted a simple commercially available 3 W mercury lamp to one of the flanges of the chamber. The UV light from the lamp creates oxygen radicals (while generating ozone as an intermediate step) from the air in the chamber and is also absorbed by the contaminants, helping the cleaning process. A more detailed description of the method can be found in [16]. It took 20 h to completely clean a contaminated mirror, while its reflectivity improved by 12% back to its original value. Results are shown in Fig. 4(c).

B. RF Plasma Source Cleaning

With the RF source, we evacuated the chamber and ran a cleaning cycle with an Evactron E50 RF plasma source mounted on a flange. It took 4 h to completely clean a contaminated mirror, while the reflectivity improved by 35% back to its original value. The improvement in reflectivity is shown in Fig. 4(b), and a visual comparison under a microscope is shown in Fig. 5.

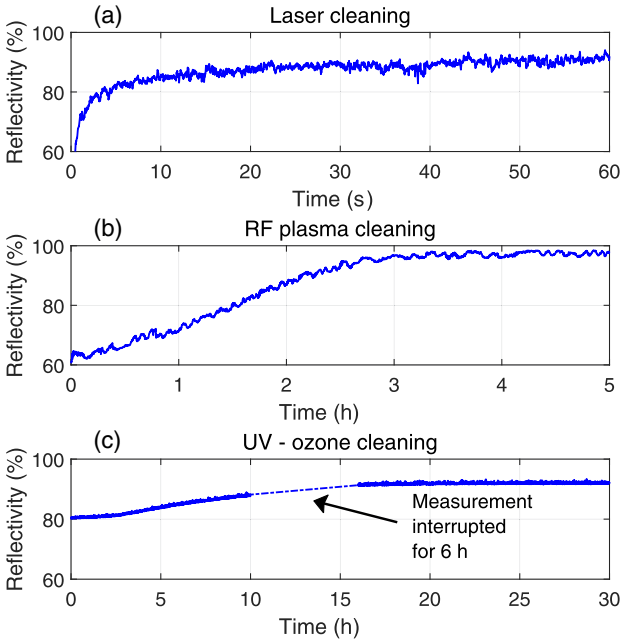

Fig. 4. Results of three LIC cleaning methods from three different mirrors in a dedicated small chamber, arranged from the fastest method on top. Although the laser cleaning seems faster (time scale in seconds), it would later require scanning the whole surface area affected by LIC. Microscope details of the surface cleaned by RF plasma source are shown in Fig. 5.

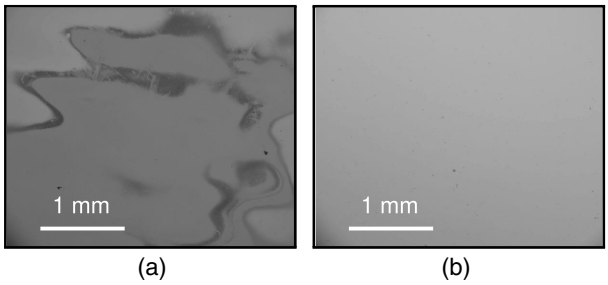

Fig. 5. Comparison of a mirror surface from a different system (beam transport of Ti:sapphire section of Prague Astrix laser system) under microscope. (a) Details of a contaminated area. (b) Same area after 5 h of RF plasma cleaning.

C. Laser Cleaning

For the laser cleaning method, we evacuated the chamber and partially filled it with oxygen (partial pressure 0.4 mbar). We irradiated the contaminated area with ultrashort pulses from a coherent Astrella laser with a fluence of 35 mJ/cm^2, repetition rate of 1 kHz, pulse duration of 50 fs, and central wavelength of 800 nm. The laser spot had a 500 μm 1/e^2 diameter. It took only 1 min to completely clean a contaminated spot on the mirror, while the reflectivity of the spot improved by 45% back to its original value, as shown in Fig. 4(a). Contrary to the other two cleaning methods mentioned in this section, removing the whole contamination would later require scanning across the contaminated surface. With LIC spots as big as 800 mm^2 on the gratings, it would take more than 16 h to clean with the cleaning laser spot of the same size.

Using this method for cleaning the contaminated optics in the Allegra system vacuum chambers, by reaching similar conditions (partial atmosphere or oxygen pressure and intensities of ∼1 TW/cm^2) and utilizing the same laser beam, which causes the LIC in the first place, is not feasible for our system at the moment. The slower cleaning rate, due to lower intensities (see Table 1), possible self-focusing, due to the partial pressure in the chambers and plasma generation due to the presence of foci in the imaging system, did not justify the risks involved. Instead, due to its simplicity and ease of use, we chose the RF plasma source as the most suitable method for cleaning optics in the Allegra vacuum chambers.

3. *IN SITU* TEST OF LIC REMOVAL

For the *in situ* test, we chose to characterize one of the dielectric gratings from a compressor inside the pump pulse compressor chamber [marked as (1) in the layout in Fig. 6]. The original average diffraction efficiency of the grating was 97%. This grating is hit by the laser pulse twice: first on its way in, while still stretched, and then once again on the way out where the pulse is compressed. No LIC is observed where the stretched pulse hits the grating, while LIC is clearly visible where the pulse is compressed. This is shown in Fig. 1.

The RF plasma source was mounted to the top of the chamber with the flange being roughly 60 cm away from surface of the grating with the LIC spot.

To test the effectiveness, we ran the RF source *in situ*. To evaluate the level of LIC on the grating after each cleaning iteration, we measured the diffraction efficiency of the −1st and 0th order across the spot with the LIC. For that, we used a small 1030 nm CW beam and moved the grating on a translation stage, as depicted in Fig. 7. After the measurement, we returned

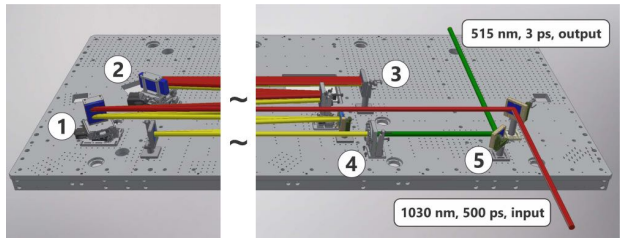

Fig. 6. Compressor layout inside the chamber: 1) first diffraction grating; 2) second diffraction grating; 3) end mirror, which folds the beam back through the compressor under a slightly different angle, resulting in two distinct laser spots on both gratings where the laser beam hits both gratings; 4) SHG crystal; 5) dichroic mirror separating 515 nm from residual 1030 nm.

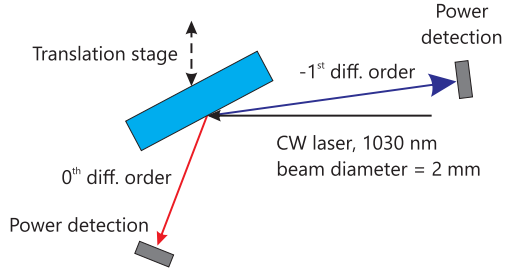

Fig. 7. Diffraction efficiency measurement layout.

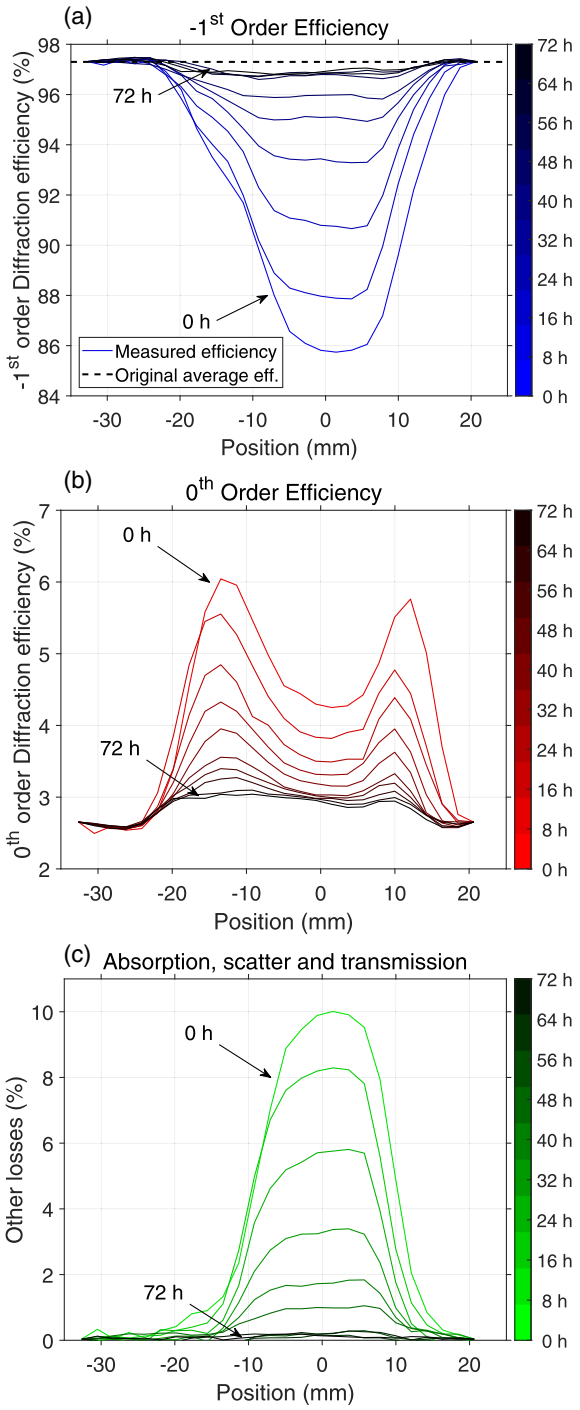

Fig. 8. Experimental data with the dielectric grating from the compressor chamber, using nine cycles (8 h each) of RF plasma source cleaning. (a) Evolution of the −1st order diffraction efficiency. (b) Evolution of the 0th order diffraction efficiency. (c) Other losses besides reflection calculated from (a) and (b).

the grating to its mount in the chamber, evacuated the chamber to $\sim 10^{-6}$ mbar, and ran the 8 h RF plasma cleaning cycle while running the turbomolecular pump at maximum speed. After this cleaning cycle, the grating was removed and measured again. This process was repeated nine times, until the diffraction efficiency in the center of the LIC spot no longer improved, as shown in Fig. 8.

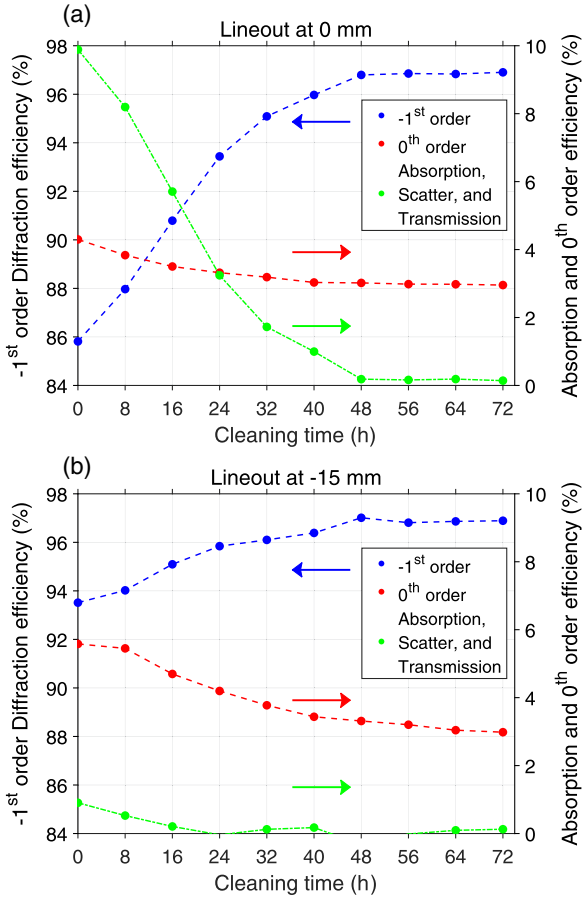

Fig. 9. Lineouts at two different positions from Fig. 8. (a) At 0 mm, indicating the center of the LIC spot where the change of the −1st order diffraction efficiency and other losses are more pronounced. (b) At −15 mm, indicating the center of the left peak in 0th order diffraction.

The data show that the "donut" shape of the LIC influences mainly the 0th order efficiency, which is larger on the edges of the LIC spot. The reason for this shape is not clear at the moment and will be the subject of future investigation. Apart from this, the overall diffraction efficiency of the −1st order is lower mainly in the center due to the absorption caused by the carbon layer. Most of the improvement occurred in the first 48 h of the cleaning cycle, as shown in Fig. 9(a), which illustrates the progress of the efficiency of −1st and 0th order and the calculated absorption during the cleaning process. RF plasma cleaning improved the diffraction efficiency of the −1st order by 13%, after which the LIC spot visually disappeared.

A. RF Source Placement Consideration

After 72 h of cleaning cycles, the LIC from the gratings was removed; however, the LIC on the dichroic mirror, which was positioned on the other side of the same chamber, did not disappear. This suggests the RF plasma cleaning is a viable solution only for the optical surfaces close to the RF source itself, probably due to the lower concentration of radicals farther from the plasma source. Other components in the chamber, which can block optical surfaces from the plasma source, may also decrease the efficiency of the cleaning. In addition, the placement of the

turbomolecular pump (in our case at the center bottom of the chamber) is important. It influences the cleaning efficiency of surfaces on the other side of the chamber as the generated ions are drifting from the RF plasma source toward the pump.

All this should be taken into consideration when choosing the method of cleaning or, in our case, the placement of the RF plasma source. For instance, in order to clean the dichroic mirror, the RF source needed to be placed on the other side of the chamber, closer to the mirror itself.

4. CONCLUSION

We identified LIC to be a problem for optical surfaces in vacuum in the Allegra laser system. Visible contamination was present only on the surfaces with compressed (<3 ps) laser pulses with intensities higher than 30 GW/cm^2. The wavelength of the laser does not play a significant role, as the contamination was observed for wavelengths at 515, 830, and 1030 nm. Based on the lack of LIC in other high-intensity lasers at ELI, average power and high repetition rate appear to be a factor in the deposition along with high intensity. The influence of LIC presence and its removal on the laser-induced damage threshold was not measured and would require a separate study.

We concluded that the RF source is a suitable solution to avoid problems with LIC in the future if the cleaning runs are scheduled regularly.

Funding. European Regional Development Fund (ADONIS, CZ.02.1.01/0.0/0.0/16–019/0000789); Ministry of Education, Youth, and Sports of the Czech Republic (NPS II Project No. LQ1606).

Disclosures. The authors declare no conflicts of interest.

REFERENCES

1. S. Toth, T. Stanislauskas, I. Balciunas, R. Budriunas, J. Adamonis, R. Danilevicius, K. Viskontas, D. Lengvinas, G. Veitas, D. Gadonas, A. Varanavičius, J. Csontos, T. Somoskoi, L. Toth, A. Borzsonyi, and K. Osvay, "SYLOS lasers–the frontier of few-cycle, multi-TW, kHz lasers for ultrafast applications at extreme light infrastructure attosecond light pulse source," J. Phys. Photon. **2**, 045003 (2020).
2. R. Antipenkov, F. Batysta, R. Boge, E. Erdman, M. Greco, J. T. Green, Z. Hubka, L. Indra, K. Majer, T. Mazanec, P. Mazůrek, J. Naylon, J. Novák, V. Šobr, A. Špaček, M. Torun, B. Tykalewicz, P. Bakule, and B. Rus, "The current commissioning results of the Allegra kilohertz high-energy laser system at ELI-beamlines," in *Laser Congress 2019 (ASSL, LAC, LS&C)* (Optical Society of America, 2019), paper ATh1A.6.
3. P. Zhang, Y. Jiang, J. Wang, W. Fan, X. Li, and J. Zhu, "Improvements in long-term output energy performance of Nd:glass regenerative amplifiers," High Power Laser Sci. Eng. **5**, e23 (2017).
4. R. B. Gillette, J. R. Hollahan, and G. L. Carlson, "Restoration of optical properties of surfaces by radiofrequency-excited oxygen," J. Vac. Sci. Technol. **7**, 534–537 (1970).
5. K. Boller, R.-P. Haelbich, H. Hogrefe, W. Jark, and C. Kunz, "Investigation of carbon contamination of mirror surfaces exposed to synchrotron radiation," Nucl. Instrum. Methods Phys. Res. **208**, 273–279 (1983).
6. E. D. Johnson and R. F. Garrett, "In situ reactive cleaning of x-ray optics by glow discharge," Nucl. Instrum. Methods Phys. Res. A **266**, 381–385 (1988).
7. R. A. Rosenberg and D. C. Mancini, "Deposition of carbon on gold using synchrotron radiation," Nucl. Instrum. Methods Phys. Res. A **291**, 101–106 (1990).
8. B. R. Müller, J. Feldhaus, F. Schäfers, and F. Eggenstein, "Cleaning of carbon contaminated vacuum ultraviolet-optics: influence on surface roughness and reflectivity," Rev. Sci. Instrum. **63**, 1428–1431 (1992).
9. P. Yadav, M. Modi, M. Swami, and P. Singh, "Ex-situ characterization of synchrotron radiation induced carbon contamination on LiF window," J. Electron Spectrosc. Relat. Phenom. **211**, 64–69 (2016).
10. D. Kokkinos, H. Schröder, K. Fleury-Frenette, M. Georges, W. Riede, G. Tzeremes, and P. Rochus, "Laser optics in space failure risk due to laser induced contamination," CEAS Space J. **9**, 153–162 (2016).
11. J. T. Hollenshead, L. E. Klebanoff, and G. Delgado, "Predicting radiation-induced carbon contamination of EUV optics," J. Vac. Sci. Technol. B **37**, 021602 (2019).
12. H. D. Wanzenboeck, P. Roediger, G. Hochleitner, E. Bertagnolli, and W. Buehler, "Novel method for cleaning a vacuum chamber from hydrocarbon contamination," J. Vac. Sci. Technol. A **28**, 1413–1420 (2010).
13. R. R. Kunz, V. Liberman, and D. K. Downs, "Experimentation and modeling of organic photocontamination on lithographic optics," J. Vac. Sci. Technol. B **18**, 1306–1313 (2000).
14. W. Riede, P. Allenspacher, H. Schröder, D. Wernham, and Y. Lien, "Laser-induced hydrocarbon contamination in vacuum," Proc. SPIE **5991**, 59910H (2006).
15. R. Schäfer, G. Schmidtke, T. Strahl, M. Pfeifer, and R. Brunner, "EUV data processing methods of the solar auto-calibrating EUV spectrometers (SolACES) aboard the International Space Station," Adv. Space Res. **59**, 2207–2228 (2017).
16. N. Bartels, P. Allenspacher, W. Riede, H. Schröder, and D. Wernham, "Removal of laser-induced contamination on ALADIN laser optics by UV/ozone cleaning," Proc. SPIE **11173**, 98–107 (2019).
17. F. E. Hovis, B. A. Shepherd, C. T. Radcliffe, A. L. Bailey, and W. T. Boswell, "Optical damage at the part per million level: the role of trace contamination in laser-induced optical damage," Proc. SPIE **2114**, 145–153 (1994).
18. S. Becker, A. Pereira, P. Bouchut, F. Geffraye, and C. Anglade, "Laser-induced contamination of silica coatings in vacuum," Proc. SPIE **6403**, 189–200 (2007).
19. T. Koide, T. Shidara, K. Tanaka, A. Yagishita, and S. Sato, "In situ DC oxygen-discharge cleaning system for optical elements," Rev. Sci. Instrum. **60**, 2034–2037 (1989).
20. R. Vane, "Immobilization and removal of hydrocarbon contamination using the Evactron® de-contaminator," Microsc. Microanal. **12**, 1662–1663 (2006).
21. S. Georgiou, "Laser Cleaning Methodologies of Polymer Substrates," in *Polymers and Light. Advances in Polymer Science*, (Springer, 2004), pp. 1–50.
22. O. Hort, M. Albrecht, V. Nefedova, O. Finke, D.-D. Mai, S. Reyné, F. Giambruno, F. Frassetto, L. Poletto, J. Andreasson, G. Julien, S. Sebban, and J. Nejdl, "High-flux source of coherent XUV pulses for user applications," Opt. Express **27**, 8871–8883 (2019).
23. F. Batysta, R. Antipenkov, J. T. Green, J. A. Naylon, J. Novák, T. Mazanec, P. Hříbek, C. Zervos, P. Bakule, and B. Rus, "Pulse synchronization system for picosecond pulse-pumped OPCPA with femtosecond-level relative timing jitter," Opt. Express **22**, 30281–30286 (2014).
24. M. Horáček, L. Indra, J. T. Green, J. A. Naylon, B. Tykalewicz, J. Novák, F. Batysta, T. Mazanec, J. Horáček, R. Antipenkov, Z. Hubka, R. Boge, P. Bakule, and B. Rus, "Multi-channel, fiber-based seed pulse distribution system for femtosecond-level synchronized chirped pulse amplifiers," Rev. Sci. Instrum. **88**, 013109 (2017).
25. R. Boge, J. Horáček, P. Mazůrek, J. A. Naylon, J. T. Green, Z. Hubka, V. Šobr, J. Novák, F. Batysta, R. Antipenkov, P. Bakule, and B. Rus, "Robust method for long-term energy and pointing stabilization of high energy, high average power solid state lasers," Rev. Sci. Instrum. **89**, 023113 (2018).
26. F. R. Wagner, G. G. El Reaidy, D. Faye, and J. Y. Natoli, "Laser induced deposits in contaminated vacuum environment: optical properties and lateral growth," Opt. Laser Technol. **122**, 105889 (2020).
27. "LIGO document E080177-v2: RGA test qualification of components for the LIGO UHV," 2020, https://dcc.ligo.org/LIGO-E080177/public.
28. J. Hřebíček, B. Rus, J. C. Lagron, J. Polan, T. Havlíček, T. Mocek, J. Nejdl, and M. Pešlo, "25 TW Ti:sapphire laser chain at PALS," Proc. SPIE **8080**, 142–148 (2011).